

000 SEMI-SUPERVISED DISEASED DETECTION FROM 001 SPEECH DIALOGUES WITH MULTI-LEVEL DATA MOD- 002 ELING 003

006 **Anonymous authors**

007 Paper under double-blind review

011 ABSTRACT

013 Detecting medical conditions from speech acoustics is fundamentally a weakly-
014 supervised learning problem: a single, often noisy, session-level label must be
015 linked to nuanced patterns within a long, complex audio recording. This task is
016 further hampered by severe data scarcity and the subjective nature of clinical an-
017 notations. While semi-supervised learning (SSL) offers a viable path to leverage
018 unlabeled data, existing audio methods often fail to address the core challenge
019 that pathological traits are not uniformly expressed in a patient’s speech. We
020 propose a novel, audio-only SSL framework that explicitly models this hierar-
021 chy by jointly learning from frame-level, segment-level, and session-level repre-
022 sentations within unsegmented clinical dialogues. Our end-to-end approach dy-
023 namically aggregates these multi-granularity features and generates high-quality
024 pseudo-labels to efficiently utilize unlabeled data. Extensive experiments show
025 the framework is model-agnostic, robust across languages and conditions, and
026 highly data-efficient—achieving, for instance, 90% of fully-supervised perfor-
027 mance using only 11 labeled samples. This work provides a principled ap-
028 proach to learning from weak, far-end supervision in medical speech analy-
029 sis. The code is available at https://anonymous.4open.science/r/semi_pathological-93F8.

031 1 INTRODUCTION

033 The use of speech acoustics as a biomarker for disease detection presents a compelling yet challeng-
034 ing machine learning problem (Strimbu & Tavel, 2010; Calif, 2018). The core task is to learn a
035 function that maps a raw audio signal, which is a complex, high-dimensional time series, to a clini-
036 cal label. However, this problem is characterized by several fundamental constraints that complicate
037 standard supervised learning approaches. First, the field is plagued by severe data scarcity. An-
038notating medical speech data requires costly expert knowledge from clinicians, making large-scale
039 dataset collection difficult (Niu et al., 2023; Koops et al., 2023; Wu et al., 2023a). Second, the labels
040 themselves are often inherently noisy. Clinical ratings, such as depression severity scores, can suffer
041 from significant inter-rater subjectivity, meaning the supervision signal is not a ground-truth value
042 but a noisy human assessment (Berisha & Liss, 2024).

043 The most distinctive challenge is the problem of weak, far-end supervision. In a typical screening
044 scenario, a single label (e.g., “depressed” or “not depressed”) is provided for an entire multi-turn
045 conversation. This session-level label is the only direct supervision signal. However, to model the
046 conversation, the audio must be processed into a sequence of fine-grained representations (e.g., at the
047 frame or clip level). A critical modeling assumption is that the pathological state is not uniformly
048 expressed throughout the session; a patient may not reveal symptomatic speech patterns in every
049 line of response. Thus, the model must learn to identify the most salient, discriminative segments
050 within a long sequence that led to the overall clinical assessment, without any direct segment-level
051 guidance (Zolnoori et al., 2023; Agbavor & Liang, 2022; Martínez-Nicolás et al., 2021).

052 Existing methods often sidestep this granularity issue by segmenting long recordings and treating
053 each segment as an independent sample (Wu et al., 2023b; Cheong et al., 2025; Li et al., 2025a),
implicitly assuming uniform expression of symptoms—an assumption that is frequently invalid (Li

et al., 2025b; Han et al., 2023). Furthermore, the significant domain shift between general speech tasks and clinical applications hinders the direct transfer of existing semi-supervised learning frameworks (Diao et al., 2023; Park et al., 2020).

To address these core machine learning challenges, we propose a novel semi-supervised framework designed for audio-based medical detection. Our approach explicitly models the hierarchy of information in a clinical conversation: from frame-level acoustics to clip-level utterances to the final session-level diagnosis. We introduce a method to dynamically aggregate and weight these multi-granularity representations to match the far-end supervision signal, effectively learning to pinpoint critical segments within a session. By leveraging unlabeled data and explicitly modeling the sparse nature of symptomatic expressions, our method achieves robust performance even with extremely limited and noisy labeled data.

Experiments on two datasets incorporating depression and Alzheimer’s detection demonstrate that with only approximately 11 labeled samples, our method can achieve 90% of the performance attained using the full training dataset. We further validate its effectiveness across diverse languages, medical conditions, and speech encoders, showing it matches fully-supervised performance using only 30% of the labels. A key feature of our method is its ability to dynamically generate high-quality pseudo-labels during training, efficiently leveraging unlabeled data without additional inference cost. This design enhances robustness, facilitates cross-lingual application, and aligns closely with real-world clinical scenarios. The main contributions of our work are as follows:

- We propose a novel, audio-only, model-agnostic semi-supervised learning framework for medical diagnosis from spoken dialogues. This framework is capable of simultaneously modeling data at multiple granularities, thereby enabling more comprehensive data utilization.
- We introduce a single-stage, end-to-end semi-supervised training method based on this framework. This approach processes complete long-form audio dialogues in a single pass and performs online updates of pseudo-labels to better leverage unlabeled data, all without incurring additional inference cost.
- We validate the effectiveness of our method across diverse languages, medical conditions, and speech encoder models. Our experiments demonstrate that with only 30% of the labeled data, our approach achieves performance comparable to its fully supervised counterpart trained on 100% of the data.

2 PROBLEM STATEMENT

This section provides a formal definition of the semi-supervised pathology detection task for speech-based clinical dialogues (illustrated in Figure 1). We begin by outlining the core formulation and the primary challenges inherent to this learning paradigm.

The problem is initially formulated as a C class semi-supervised classification problem, where one class represents healthy participants and the remaining $C-1$ classes correspond to specific pathological conditions.

The labeled and unlabeled datasets are denoted as $\mathcal{D}_L = \{\mathbf{x}_i^l, \mathbf{y}_i^l\}_{i=1}^{N_L}$ and $\mathcal{D}_U = \{\mathbf{x}_i^u\}_{i=1}^{N_U}$, respectively, where both $\mathbf{x}_i^l \in R^{t_i \times d}$ and $\mathbf{x}_i^u \in R^{t_i \times d}$ are speech-based clinical dialogue samples of varying lengths (Chen et al., 2023a). Generally, the duration of each sample varies and exhibits significant variance. N_L and N_U represent the number of samples in the labeled and unlabeled data, respectively. The term $y \in \{0, 1, 2, \dots, C-1\}$ is the one-hot ground truth label, which is exclusively available for the labeled data and indicates the class of the sample.

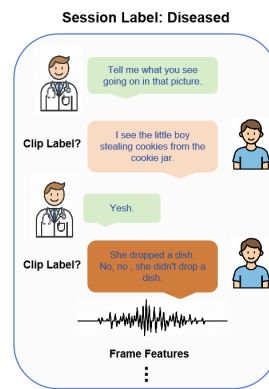


Figure 1: Pathological speech detection in clinical diagnostic dialogues.

108 For each sample $x_i \in \{D_L, D_U\}$ in the labeled and unlabeled data:

109
110
$$x_i = \{R_{i,1}, R_{i,2}, R_{i,3}, \dots, R_{i,n}\} \quad (1)$$

111
112
113
$$R_{i,j} = \{W_1^{S_1}, W_2^{S_2}, W_3^{S_3}, \dots, W_m^{S_m}\} \quad (2)$$

114 Here, $R_{i,j}$ denotes the j -th dialogue session in the i -th sample, and $W_k^{S_k}$ represents the k -th
115 utterance from speaker $S_k \in \{\text{INV}, \text{PAR}\}$ within that session. The speakers consisted of inves-
116 tigators and participants. The variable n is the total number of dialogue sessions in the sample x_i ,
117 while m is the number of utterances in a given session. Notably, the utterances within each dialogue
118 session are sequentially ordered. In contrast, different dialogue sessions are mutually independent,
119 and thus no specific order is maintained among them. This formulation presents several fundamental
120 challenges:

121
122
123
124
125
126
127
128
129
130
131
132
133
134
135

- **Data Scarcity and Noisy Labels:** The labeled set \mathcal{D}_L is typically small due to the high cost of clinical annotations. Furthermore, the labels themselves often exhibit significant noise and subjectivity due to inter-rater variance in clinical assessments.
- **Session-Level Supervision with Sparse Manifestations:** Each dialogue session x_i receives only a single global label y_i , despite consisting of thousands of acoustic frames and multiple conversational turns. Critically, pathological speech patterns may be *sparsely distributed* throughout the session—patients do not necessarily exhibit disease markers in every utterance or response.
- **Granularity Mismatch:** The supervision signal operates at the session level, while meaningful acoustic features must be extracted at much finer temporal resolutions (frame-level or clip-level). The model must therefore learn to identify which specific segments within a long dialogue are most indicative of the overall pathological condition, without explicit segment-level guidance.

136 These challenges necessitate a learning framework that can handle weak, far-end supervision while
137 effectively leveraging unlabeled data to overcome annotation scarcity.

139 3 METHODS

140 We propose a novel semi-supervised learning framework that hierarchically models speech data at
141 three distinct granularities: session, clip, and frame levels (Figure 2). At the session-level, which
142 constitutes the main pipeline of our framework, the model is designed to process the entire audio
143 sample x . We adopt an architecture commonly used in instance learning, where each utterance $W_k^{S_k}$
144 is encoded individually. Subsequently, a multi-head attention mechanism is employed to aggregate
145 the features of each utterance. The resulting representation is then fed into a downstream detection
146 task to yield the final result.

147 At the clip-level, the model trained in the main pipeline is leveraged to generate pseudo-labels for
148 each utterance $W_k^{S_k}$. These pseudo-labels are then used to further train the audio encoder. This
149 process enables the model to effectively capture the characteristics of each utterance in the dialogue,
150 thereby facilitating the learning of sentence-level features by the audio encoder.

151 At the frame-level, we apply a Siamese network paradigm. By employing a contrastive loss, the
152 model is trained to perform finer-grained modeling of frame-level features.

153 3.1 SESSION-LEVEL

154 The primary workflow of our framework, highlighted in green in Figure 2, processes an entire sample
155 x to produce the final detection result. To address the memory constraints of loading a complete
156 sample at once, we partition each sample $x_i = \{\text{clip}_1, \text{clip}_2, \text{clip}_3, \dots, \text{clip}_n\}$ into n clips. Each
157 $\text{clip}_i \in R^{t_i}$ is a vector sequence with a temporal length of t_i . Each clip_i is then individually fed
158 into an audio encoder E , to generate a corresponding embedding, $\text{embed}_i \in R^{t_i \times d}$. The resulting

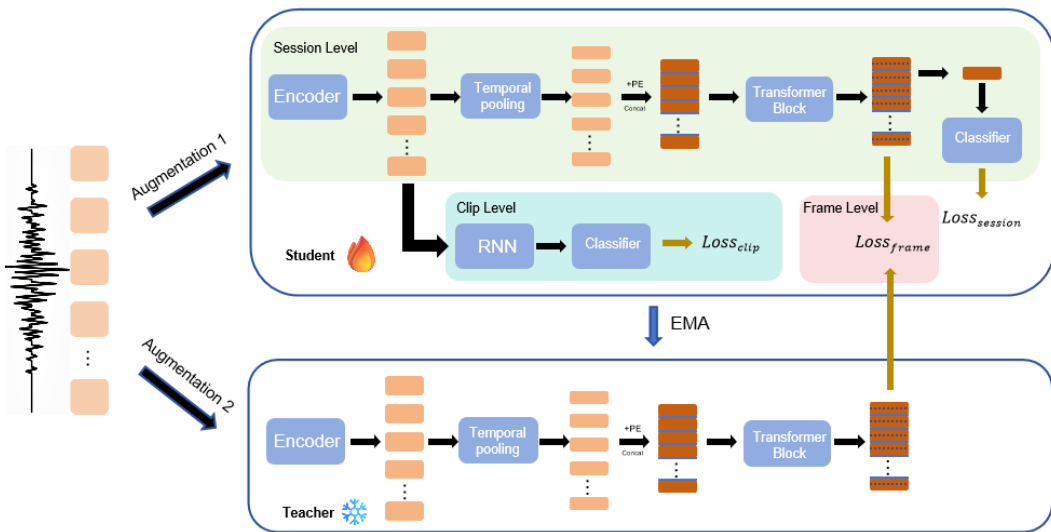


Figure 2: Model architecture overview. Our framework operates at three hierarchical levels: **session-level** (global dialogue representation via Transformer), **clip-level** (utterance-level modeling via RNN with pseudo-labels), and **frame-level** (acoustic feature consistency via MSE loss). The teacher-student framework with Exponential Moving Average (EMA) updates enables dynamic pseudo-label refinement during training.

embeddings may have varying temporal lengths t but share a constant feature dimension d . For the audio encoder, standard architectures such as wav2vec2 (Baevski et al., 2020), HuBERT (Hsu et al., 2021), or WavLM (Chen et al., 2022) can be employed. To further reduce the data scale, the embedding $embed_i$ may optionally be passed through a temporal pooling layer, yielding a more compact representation, $embed_i$. Note that this step only reduces the temporal dimension t , while the feature dimension d is preserved.

Following these steps, we obtain an encoded representation for each clip:

$$embed_{clip_i} = POOL(E(clip_i)) \quad (3)$$

Subsequently, learnable positional encodings are added to the clip-level embeddings. The clip-level embeddings $embed_{clip}$ are first concatenated in their original sequential order to form a session-level embedding. This embedding is subsequently fed into a multi-layer transformer (Vaswani et al., 2017) to produce the final session-level representation $embed_{audio} \in R^{t \times d}$. Building upon this representation, a sample-level embedding is derived by aggregating features along the temporal dimension. This can be accomplished either by adding an additional layer to model global information or by employing a temporal attention mechanism for fusion. Finally, for the specific downstream task, a simple classification head is appended to the sample-level embedding to predict the final labels. During this process, pseudo-labels are generated for unlabeled data and incorporated into the training set. The model is then trained for the detection task in a supervised manner using the cross-entropy loss function.

3.2 CLIP-LEVEL

The objective of this method is to fine-tune the session-level encoder E , enabling it to model finer-grained data at the clip-level. This process is illustrated by the blue-highlighted portion of Figure 2. Specifically, the embeddings $embed_{clip}$ obtained from the session-level, optionally after a pooling operation, are fed as a sequence into a Recurrent Neural Network (RNN). Since a clip-level segment typically corresponds to a short sequence, such as a single utterance or a fixed-duration speech segment, standard RNN architectures like Gated Recurrent Units (Chung et al., 2014) or Long Short-Term Memory (Hochreiter & Schmidhuber, 1997) are employed to process this sequence and generate the final clip-level embedding:

216
217
218

$$embed_{clip_i} = RNN(clip_i) \quad (4)$$

219 The clip-level pseudo-labels are obtained directly from the main session-level pipeline and are sub-
220 sequentially used to supervise the training via a cross-entropy loss function. In contrast to prior work,
221 this approach avoids the strong assumption that every utterance from a patient exhibits patholog-
222 ical features, while every utterance from a healthy individual is devoid of them. Moreover, this
223 method can be trained on data containing dialogue from both investigators and participants, without
224 requiring the explicit extraction of the participant’ utterances.

225 3.3 FRAME-LEVEL

226 The objective of this method is to enable the model to capture finer-grained features at the frame
227 level. To this end, we employ a siamese network paradigm, which consists of a student and a
228 teacher model that share an identical architecture (The region highlighted in red in Figure 2.). The
229 parameters of the teacher network are updated as an Exponential Moving Average (EMA) of the
230 student network’s parameters:

$$\theta_{teacher} \leftarrow m \cdot \theta_{teacher} + (1 - m) \cdot \theta_{student} \quad (5)$$

231 Throughout the training process, the teacher network remains frozen; no gradients are backprop-
232 agated through it, and only the student network is trained. For a given input x , we generate two
233 distinct views by applying different data augmentations (one of which may be the identity trans-
234 formation). These views are then fed into the teacher and student networks, respectively. The aug-
235 mentation strategy employs common audio techniques such as speed perturbation, pitch shifting,
236 and time masking. After being processed by the session-level pipeline of each network, we obtain
237 the embeddings $embed_{teacher}$, $embed_{student} \in R^{t \times d}$. Since these embeddings originate from the
238 same sample, the objective is to enforce consistency between them. The loss function is therefore
239 defined as:

$$Loss_{frame} = MSELoss(embed_{teacher}, embed_{student}) \quad (6)$$

244 3.4 ONLINE SINGLE-STAGE TRAINING RECIPE

245 In contrast to conventional multi-stage semi-supervised learning methods, our approach operates
246 in a single stage, facilitating the online update of pseudo-labels. During the training process, after
247 an initial warm-up period of k_0 steps, all pseudo-labels at both the audio- and clip-levels are re-
248 evaluated and updated every k steps. This update mechanism employs a threshold-based strategy:
249 unlabeled samples with model-predicted confidence scores exceeding a predefined threshold are
250 incorporated into the training set for the subsequent k steps. Conversely, samples with scores below
251 the threshold are excluded from (or optionally retained in) the training set for this duration.

252 In summary, the total loss for each training iteration is computed as a weighted sum of three dis-
253 tinct level-specific losses. The parameters of the teacher model are subsequently updated using the
254 parameters of the student model. The loss function is defined as:

$$Loss = \alpha Loss_{session} + \beta Loss_{clip} + \gamma Loss_{frame} \quad (7)$$

255 where α , β , and γ are the weighting coefficients for the respective loss components.

256 4 EXPERIMENTAL SETUP

257 To validate the efficacy of our proposed method, we conducted experiments targeting two distinct
258 pathological conditions: **Depression** and **Alzheimer’s disease**, using publicly available datasets in
259 different languages. We evaluated our method under semi-supervised settings with varying propor-
260 tions of labeled data, employing the Macro F1 Score to address class imbalance. Comprehensive
261 ablation studies were performed to analyze the contribution of each component, and we compare

270 our approach against relevant baselines despite the limited prior work in audio-only semi-supervised
 271 pathology detection.
 272

273 **Datasets** To ensure fair comparison with prior work, we followed the same evaluation protocols
 274 established in the original dataset publications. Detailed dataset statistics, preprocessing steps, and
 275 experimental configurations are provided in Appendix A.
 276

- 277 • **Depression Detection:** A Chinese EATD-Corpus dataset (Shen et al., 2022) of 162 partic-
 278 ipants (30 depressed), with 3-fold cross-validation.
- 279 • **Alzheimer’s Detection:** An English ADReSSo21 dataset (Luz et al., 2021) with standard
 280 train/test splits. The dataset comprises a total of 237 samples, including 122 positive sam-
 281 ples.
 282

283 **Evaluation Protocol** We adopted the Macro $F1$ Score as our primary metric to mitigate the effects
 284 of class imbalance, particularly relevant for the depression detection task. For the semi-supervised
 285 evaluation, we conducted experiments using varying proportions of labeled data (10%, 20%, 30%,
 286 40%, 50%, and 100% of training samples) to comprehensively assess our method’s efficiency.
 287

288 **Training Details** We employed the Adam optimizer with an initial learning rate of 2e-6 and a
 289 weight decay of 1e-8. The batch sizes for both labeled and unlabeled data were set to 2, with 4
 290 gradient accumulation steps. The primary data augmentation methods included speed perturbation
 291 and time masking. The decay rate for the Exponential Moving Average (EMA) was set to 0.999.
 292 For the model architecture, features were extracted from the 10th layer of all audio encoders. The
 293 temporal pooling kernel size was set to 5. The transformer model comprised 3 blocks with 16
 294 attention heads, while the RNN model consisted of a 2-layer bidirectional LSTM. Notably, as the
 295 EATD-Corpus is a Chinese dataset, we used HuBERT and wav2vec2 models pre-trained on Chinese
 296 speech datasets. Due to the unavailability of a WavLM model pre-trained on Chinese data, the
 297 version we employed was pre-trained on an English dataset.
 298

299 5 RESULTS AND ANALYSIS

300 We evaluate our method’s performance under varying proportions of labeled data against a session-
 301 level baseline that excludes pseudo-labeling. The results demonstrate our framework’s effectiveness
 302 across both depression and Alzheimer’s detection tasks, as shown in Table 1.
 303

305 5.1 SEMI-SUPERVISED AND FULLY-SUPERVISED SETTING RESULTS

307 **Data Efficiency.** Our method exhibits remarkable data efficiency, achieving strong performance
 308 with limited labeled data. For depression detection, our approach attained 90% of the fully-
 309 supervised baseline’s performance using only 10% of the labels. Notably, with just 30% of the
 310 labels, it nearly matched the baseline’s performance when trained on the full dataset. Similarly, for
 311 Alzheimer’s detection, our method approached full-supervised performance with 30% of the data
 312 and surpassed it with only 40%.

313 **Performance Gains.** Significant improvements over the baseline were observed across all label
 314 proportions. In depression detection, a notable gain of 4.59% was achieved at the 50% label ratio.
 315 The most substantial improvement for Alzheimer’s detection was a 4.38% increase at the challenging
 316 10% label ratio, highlighting the method’s effectiveness in extremely low-data regimes.
 317

318 **Full Supervision Enhancement.** Crucially, our method outperformed the baseline even in the
 319 fully supervised setting (100% labels) for both disorders. This indicates that the integrated clip-
 320 level and frame-level components provide substantial performance benefits beyond pseudo-labeling,
 321 enhancing feature learning and representation robustness. These results collectively underscore
 322 the dual advantage of our framework: effectively leveraging unlabeled data to mitigate annotation
 323 scarcity while simultaneously enriching the model’s representational capacity through multi-
 granularity analysis.

324
 325 Table 1: Performance comparison of our method versus the baseline across different labeled data
 326 proportions for depression and Alzheimer’s detection. Results report Macro F1 scores (standard
 327 deviation over 3 runs) under varying supervision levels (10%-100% of labeled data).

Method	100%	50%	40%	30%	20%	10%
Depression Detection						
Baseline	59.53(1.51)	57.41(5.48)	55.78(7.14)	56.04(7.98)	55.00(7.25)	51.73(2.39)
Ours	63.26(1.34)	62.00(5.39)	58.51(9.00)	58.59(9.16)	57.70(9.07)	54.37(3.79)
Alzheimer’s Detection						
Baseline	71.25(1.42)	70.18(1.12)	69.80(1.47)	67.79(1.49)	67.45(0.56)	65.09(0.55)
Ours	73.01(0.60)	71.35(0.60)	72.14(1.46)	70.11(0.52)	69.80(0.56)	69.47(0.62)

335
 336 **Comparisons with existing works.** Additionally, we compare our method’s fully-supervised per-
 337 formance against existing approaches to establish its competitiveness. As shown in Table 2 and Ta-
 338 ble 3, our method achieves performance comparable to state-of-the-art methods on both depression
 339 and Alzheimer’s detection tasks, despite not being specifically optimized for the fully-supervised
 340 setting.

341
 342 Table 2: Comparison on depression de-
 343 tection. Methods marked with * = re-
 344 ported in original publications.

	F1 Score
CAMFM*(Xue et al., 2024)	0.73
ACMA*(Iyortsuun et al., 2024)	0.65
DepressGEN*(Liang et al., 2025)	0.69
Ours	0.68

345 Table 3: Comparison on Alzheimer’s
 346 detection. Methods marked with * = re-
 347 ported in original publications.

	F1 Score
Whisper-TL*Wu et al. (2024)	0.77
CogniAlign*Ortiz-Perez et al. (2025)	0.80
Wu et al. (2024)*	0.86
Ours	0.83

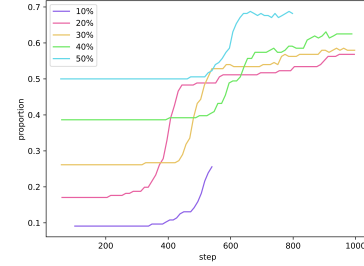
350 **Pseudo-label Analysis.** We analyze the evolution of pseudo-label quality throughout training
 351 in Figure 3, showing a consistent upward trend in the proportion of correctly labeled samples
 352 as the model converges. Our method can generate progressively higher-quality pseudo-labels.
 353 Notably, in later training stages, the pseudo-label accuracy for the 20% - 40% labeled data
 354 settings surpasses the performance of the one trained with 50% ground-truth labels (Table 1).
 355 This suggests that our framework effectively
 356 creates a self-improving training cycle where
 357 pseudo-labels eventually exceed the quality of
 358 additional manual annotations.

359 Furthermore, the frame-level component pro-
 360 vides inherent robustness against pseudo-label
 361 noise. Since frame-level training operates inde-
 362 pendently of pseudo-labels and focuses on low-
 363 level acoustic patterns, it mitigates potential er-
 364 ror propagation from incorrect session-level or
 365 clip-level pseudo-labels. This multi-granularity
 366 approach creates a balanced learning system
 367 where each component complements the oth-
 368 ers’ limitations.

369 5.2 ABLATION STUDY

370 We conduct comprehensive ablation studies to validate the contributions of each component in
 371 our framework. The experiments are designed to address four key aspects: the efficacy of multi-
 372 granularity modeling, the impact of encoder trainability, the robustness to different audio encoders,
 373 and the handling of investigator speech.

374 **Multi-granularity Modeling Efficacy** Table 4 presents an incremental ablation of the three hi-
 375 erarchical components. Each level consistently contributes to performance improvements across
 376 all labeled data proportions, with the **frame-level component yielding the most significant gains**.



377 Figure 3: Evolution of pseudo-label accuracy dur-
 378 ing training on depression detection.

378 This demonstrates the importance of fine-grained acoustic analysis for pathological speech detection.
 379 In the fully-supervised setting (100% labels), where the session-level pseudo-labeling is in-
 380 active, the performance improvement validates the combined efficacy of clip-level and frame-level
 381 components.
 382

384 Table 4: Ablation study of hierarchical components on depression detection. Results show Macro F1
 385 scores (mean±std) with incremental addition of session-level, clip-level, and frame-level modules.
 386 “Ours-frozen” denotes training with frozen audio encoder.

	100%	50%	40%	30%	20%	10%
Baseline	59.53(1.51)	57.41(5.48)	55.78(7.14)	56.04(7.98)	55.00(7.25)	51.73(2.39)
+Session-level	-	60.55(6.11)	57.09(8.62)	58.25(9.55)	55.51(7.53)	52.95(3.09)
+Clip-level	60.78(4.52)	58.30(5.41)	56.11(8.34)	56.55(8.27)	55.52(7.75)	52.50(2.73)
+Frame-level	62.87(3.04)	60.31(7.33)	58.21(9.42)	58.21(9.42)	57.18(8.68)	54.21(3.17)
Ours-frozen	-	60.29(5.61)	58.07(8.97)	60.37(5.23)	56.96(5.90)	52.82(2.45)
Ours	63.26(1.34)	62.00(5.39)	58.51(9.00)	58.59(9.16)	57.70(9.07)	54.37(3.79)

393
 394 **Encoder Trainability and Component Isolation** To further isolate each component’s contribu-
 395 tion, we conducted experiments with a frozen audio encoder. Under this condition, the clip-level
 396 component (which operates directly on encoder outputs) is effectively disabled. The maintained per-
 397 formance gain demonstrates the **joint effectiveness of session-level and frame-level components**.
 398 Notably, trainable encoders generally yield greater improvements, highlighting the importance of
 399 feature adaptation for medical speech tasks.

401 Table 5: Results of different audio encoders on depression detection

	100%	50%	40%	30%	20%	10%
wav2vec2						
Baseline	61.29(4.43)	58.76(3.98)	57.89(3.53)	57.26(3.46)	54.96(0.72)	54.32(6.79)
Ours	63.43(2.92)	59.75(3.80)	60.30(3.64)	57.85(4.06)	57.82(2.93)	55.45(2.54)
WavLM						
Baseline	59.80(3.72)	56.98(6.63)	57.85(5.25)	58.31(4.16)	59.37(4.32)	53.37(7.59)
Ours	63.56(4.97)	60.39(4.63)	60.73(5.89)	59.42(5.57)	60.54(7.15)	59.62(5.22)

411 **Architectural Robustness Across Encoders** We evaluated our framework with three popular au-
 412 dio encoders: wav2vec2, HuBERT, and WavLM (Tables 5 and 6). Our method achieves consistent
 413 performance gains across all architectures, demonstrating its model-agnostic nature. An interest-
 414 ing observation emerges with WavLM on the Chinese EATD-Corpus, where performance degrades
 415 with more labeled data. We attribute this to cross-lingual transfer issues, as WavLM was primarily
 416 pre-trained on English speech, highlighting the importance of language-matched pre-training.

417 **Robustness to Investigator Speech** As shown in Table 6, our method maintains performance im-
 418 provements even when processing raw dialogues containing both participant and investigator speech.
 419 This eliminates the need for error-prone preprocessing steps like speaker diarization, making our
 420 framework more suitable for real-world clinical applications where clean speech segmentation is
 421 challenging.

424 Table 6: Different audio encoders and inclusion of investigators’ speech segments on Alzheimer’s
 425 Detection.

	100%	50%	40%	30%	20%	10%
wav2vec2						
Baseline	68.74(1.51)	65.69(1.40)	60.84(5.19)	58.74(6.09)	53.58(3.05)	50.36(10.17)
Ours	70.48(3.12)	65.91(0.83)	62.34(5.53)	64.51(2.29)	55.70(4.14)	53.61(3.01)
with investigator						
Baseline	72.84(0.54)	72.68(1.41)	70.50(1.09)	68.21(2.20)	66.25(1.63)	66.93(0.47)
Ours	73.62(0.56)	72.92(0.98)	72.44(1.07)	69.76(0.01)	70.42(1.01)	69.72(0.52)

432 6 RELATED WORK

434 Pathological speech analysis exhibits certain advantages in cross-lingual applicability and robust-
 435 ness to transcription errors. While multi-modal methods exist that combine acoustic, text, and vi-
 436 sual information (Cheong et al., 2025; Thallinger et al., 2025; Wu et al., 2024), they face significant
 437 challenges, including error propagation from automatic speech recognition systems and limited gen-
 438 eralization across languages and domains. Audio-only approaches offer a promising alternative by
 439 learning pathological patterns directly from acoustic signals. This is particularly valuable given the
 440 linguistic imbalance in available datasets, where most resources exist for high-resource languages
 441 like English and Chinese, while low-resource languages remain underserved. By bypassing linguis-
 442 tic content, these methods can achieve better cross-lingual transfer, making them more suitable for
 443 global healthcare applications.

444 However, current audio-only methods (Feng & Chaspari, 2024; Chen et al., 2023b; Zhou et al., 2022;
 445 Zhao et al., 2025) have predominantly focused on fully-supervised paradigms, typically employing
 446 transfer learning from general-purpose self-supervised audio models. The semi-supervised learning
 447 paradigm remains largely unexplored in this domain, despite its potential to address the critical chal-
 448 lenge of limited labeled medical data. This gap is particularly notable given that semi-supervised
 449 techniques have shown success in other audio domains but face unique challenges in medical ap-
 450 plications due to the sparse nature of pathological patterns in speech. Our work addresses this gap
 451 by proposing a novel semi-supervised framework specifically designed for audio-only pathological
 452 speech detection, leveraging multi-granularity analysis to effectively utilize both labeled and unla-
 453 beled data while maintaining cross-lingual applicability.

454 Semi-Supervised Learning (SSL) aims to enhance model performance by leveraging abundant un-
 455 labeled data. Prevailing methods are generally based on consistency regularization (Sohn et al.,
 456 2020), distribution alignment (Kim et al., 2020), and contrastive learning (Lee et al., 2022; Yang
 457 et al., 2022). Most of these methods focus on selecting reliable pseudo-labels throughout the train-
 458 ing process (Gan et al.). However, the direct application of these methods to the medical domain is
 459 impeded by the multi-level and hierarchical nature of clinical dialogues. Furthermore, the reliance
 460 on far-end supervision poses additional challenges to improving the quality of pseudo-labels.

461 7 LIMITATIONS

463 Despite its strong performance, our method has limitations, primarily stemming from its nature as
 464 an audio-only approach. In contrast to multimodal systems, our model cannot leverage information
 465 from other modalities. However, this unimodal design offers distinct advantages. Modeling solely
 466 on acoustic information facilitates cross-domain generalization, reduces training data requirements,
 467 and results in a more parameter-efficient model. Furthermore, it obviates challenges inherent in
 468 multimodal approaches, such as potential modality conflicts.

470 8 CONCLUSION

472 In this work, we propose a novel, audio-only semi-supervised learning framework for medical diag-
 473 nosis from speech-based clinical dialogues. Our method is uniquely designed to handle long-form
 474 medical consultation dialogues, simultaneously modeling speech data at three distinct granularity
 475 levels (session, segment, and frame) to ensure comprehensive data utilization. By dynamically gen-
 476 erating high-quality pseudo-labels within a single-stage, end-to-end training process, our approach
 477 effectively leverages large volumes of unlabeled data without incurring additional inference costs.
 478 It avoids the limitations common in multi-modal methods. Our extensive experiments validate the
 479 effectiveness of the proposed framework. The efficacy of our method across diverse languages, med-
 480 ical conditions, and underlying speech encoders demonstrates its model-agnostic nature and strong
 481 generalization capability.

482 ETHICS STATEMENT

483 The authors have read and adhere to the ICLR Code of Ethics. This work does not involve human
 484 subjects, identifiable private data, or harmful applications. All datasets used are publicly available

486 and were used in accordance with their original licenses and intended purposes. No external spon-
 487 sorship or conflict of interest influenced the design or conclusions of this work.
 488

489 **REPRODUCIBILITY STATEMENT**

490 All code and source files are provided in the supplementary material and will be publicly re-
 491 leased. Additional implementation details can be found in the training details section and https://anonymous.4open.science/r/semi_pathological-93F8.
 492

493 **REFERENCES**

494

495 Felix Agbavor and Hualou Liang. Predicting dementia from spontaneous speech using large lan-
 496 guage models. *PLOS digital health*, 1(12):e0000168, 2022.

497 Alexei Baevski, Yuhao Zhou, Abdelrahman Mohamed, and Michael Auli. wav2vec 2.0: A frame-
 498 work for self-supervised learning of speech representations. *Advances in neural information*
 499 *processing systems*, 33:12449–12460, 2020.

500 Visar Berisha and Julie M Liss. Responsible development of clinical speech ai: Bridging the gap
 501 between clinical research and technology. *NPJ digital medicine*, 7(1):208, 2024.

502 Robert M Califf. Biomarker definitions and their applications. *Experimental biology and medicine*,
 503 243(3):213–221, 2018.

504 Hao Chen, Ran Tao, Yue Fan, Yidong Wang, Jindong Wang, Bernt Schiele, Xing Xie, Bhiksha Raj,
 505 and Marios Savvides. Softmatch: Addressing the quantity-quality trade-off in semi-supervised
 506 learning. *arXiv preprint arXiv:2301.10921*, 2023a.

507 Sanyuan Chen, Chengyi Wang, Zhengyang Chen, Yu Wu, Shujie Liu, Zhuo Chen, Jinyu Li, Naoyuki
 508 Kanda, Takuwa Yoshioka, Xiong Xiao, et al. Wavlm: Large-scale self-supervised pre-training for
 509 full stack speech processing. *IEEE Journal of Selected Topics in Signal Processing*, 16(6):1505–
 510 1518, 2022.

511 Weidong Chen, Xiaofen Xing, Xiangmin Xu, Jianxin Pang, and Lan Du. Speechformer++: A
 512 hierarchical efficient framework for paralinguistic speech processing. *IEEE/ACM Transactions*
 513 *on Audio, Speech, and Language Processing*, 31:775–788, 2023b.

514 Jiae Cheong, Aditya Bangar, Sinan Kalkan, and Hatice Gunes. U-fair: Uncertainty-based multi-
 515 modal multitask learning for fairer depression detection. *arXiv preprint arXiv:2501.09687*, 2025.

516 Junyoung Chung, Caglar Gulcehre, KyungHyun Cho, and Yoshua Bengio. Empirical evaluation of
 517 gated recurrent neural networks on sequence modeling. *arXiv preprint arXiv:1412.3555*, 2014.

518 Enmao Diao, Eric W Tramel, Jie Ding, and Tao Zhang. Semi-supervised federated learning for
 519 keyword spotting. In *2023 IEEE International Conference on Multimedia and Expo Workshops*
 520 (*ICMEW*), pp. 466–469. IEEE, 2023.

521 Kexin Feng and Theodora Chaspari. Robust and explainable depression identification from speech
 522 using vowel-based ensemble learning approaches. In *2024 IEEE EMBS International Conference*
 523 *on Biomedical and Health Informatics (BHI)*, pp. 1–8. IEEE, 2024.

524 Kai Gan, Bo Ye, Min-Ling Zhang, and Tong Wei. Semi-supervised clip adaptation by enforcing
 525 semantic and trapezoidal consistency. In *The Thirteenth International Conference on Learning*
 526 *Representations*.

527 Zhuojin Han, Yuanyuan Shang, Zhuhong Shao, Jingyi Liu, Guodong Guo, Tie Liu, Hui Ding, and
 528 Qiang Hu. Spatial-temporal feature network for speech-based depression recognition. *IEEE*
 529 *Transactions on Cognitive and Developmental Systems*, 16(1):308–318, 2023.

530 Sepp Hochreiter and Jürgen Schmidhuber. Long short-term memory. *Neural computation*, 9(8):
 531 1735–1780, 1997.

540 Wei-Ning Hsu, Benjamin Bolte, Yao-Hung Hubert Tsai, Kushal Lakhotia, Ruslan Salakhutdinov,
 541 and Abdelrahman Mohamed. Hubert: Self-supervised speech representation learning by masked
 542 prediction of hidden units. *IEEE/ACM transactions on audio, speech, and language processing*,
 543 29:3451–3460, 2021.

544 Ngumimi Karen Iyortsuun, Soo-Hyung Kim, Hyung-Jeong Yang, Seung-Won Kim, and Min Jhon.
 545 Additive cross-modal attention network (acma) for depression detection based on audio and tex-
 546 tual features. *IEEE Access*, 12:20479–20489, 2024.

548 Jaehyung Kim, Youngbum Hur, Sejun Park, Eunho Yang, Sung Ju Hwang, and Jinwoo Shin. Dis-
 549 tribution aligning refinery of pseudo-label for imbalanced semi-supervised learning. *Advances in*
 550 *neural information processing systems*, 33:14567–14579, 2020.

551 Sanne Koops, Sanne G Brederoo, Janna N de Boer, Femke G Nadema, Alban E Voppel, and Iris E
 552 Sommer. Speech as a biomarker for depression. *CNS & Neurological Disorders-Drug Targets-
 553 CNS & Neurological Disorders*, 22(2):152–160, 2023.

555 Doyup Lee, Sungwoong Kim, Ildoo Kim, Yeongjae Cheon, Minsu Cho, and Wook-Shin Han. Con-
 556 trastive regularization for semi-supervised learning. In *Proceedings of the IEEE/CVF conference
 557 on computer vision and pattern recognition*, pp. 3911–3920, 2022.

558 Yaqin Li, Chenjian Sun, and Yihong Dong. A novel audio-visual multimodal semi-supervised model
 559 based on graph neural networks for depression detection. In *ICASSP 2025-2025 IEEE Interna-
 560 tional Conference on Acoustics, Speech and Signal Processing (ICASSP)*, pp. 1–5. IEEE, 2025a.

562 Yuanchao Li, Zixing Zhang, Jing Han, Peter Bell, and Catherine Lai. Semi-supervised cognitive
 563 state classification from speech with multi-view pseudo-labeling. In *ICASSP 2025-2025 IEEE
 564 International Conference on Acoustics, Speech and Signal Processing (ICASSP)*, pp. 1–5. IEEE,
 565 2025b.

566 Wenrui Liang, Rong Zhang, Xuezhen Zhang, Ying Ma, and Wei-Qiang Zhang. Depressgen: Syn-
 567 thetic data generation framework for depression detection. In *Proc. Interspeech 2025*, pp. 464–
 568 468, 2025.

569 Saturnino Luz, Fasih Haider, Sofia De la Fuente, Davida Fromm, and Brian MacWhinney. Detecting
 570 cognitive decline using speech only: The adresso challenge. *arXiv preprint arXiv:2104.09356*,
 571 2021.

573 Israel Martínez-Nicolás, Thide E Llorente, Francisco Martínez-Sánchez, and Juan José G Meilán.
 574 Ten years of research on automatic voice and speech analysis of people with alzheimer’s disease
 575 and mild cognitive impairment: a systematic review article. *Frontiers in Psychology*, 12:620251,
 576 2021.

577 Minxue Niu, Amrit Romana, Mimansa Jaiswal, Melvin McInnis, and Emily Mower_Provost. Cap-
 578 turing mismatch between textual and acoustic emotion expressions for mood identification in
 579 bipolar disorder. In *Interspeech*. Interspeech, 2023.

581 David Ortiz-Perez, Manuel Benavent-Lledo, Javier Rodriguez-Juan, Jose Garcia-Rodriguez, and
 582 David Tomás. Cognialign: Word-level multimodal speech alignment with gated cross-attention
 583 for alzheimer’s detection. *arXiv preprint arXiv:2506.01890*, 2025.

584 Daniel S Park, Yu Zhang, Ye Jia, Wei Han, Chung-Cheng Chiu, Bo Li, Yonghui Wu, and
 585 Quoc V Le. Improved noisy student training for automatic speech recognition. *arXiv preprint
 586 arXiv:2005.09629*, 2020.

587 Ying Shen, Huiyu Yang, and Lin Lin. Automatic depression detection: An emotional audio-textual
 588 corpus and a gru/bilstm-based model. In *ICASSP 2022-2022 IEEE International Conference on
 589 Acoustics, Speech and Signal Processing (ICASSP)*, pp. 6247–6251. IEEE, 2022.

591 Kihyuk Sohn, David Berthelot, Nicholas Carlini, Zizhao Zhang, Han Zhang, Colin A Raffel,
 592 Ekin Dogus Cubuk, Alexey Kurakin, and Chun-Liang Li. Fixmatch: Simplifying semi-supervised
 593 learning with consistency and confidence. *Advances in neural information processing systems*,
 33:596–608, 2020.

594 Kyle Strimbu and Jorge A Tavel. What are biomarkers? *Current Opinion in HIV and AIDS*, 5(6):
 595 463–466, 2010.

597 Bernhard Thallinger, Laurin Wagner, Theresa Bloder, and Mario Zusag. A multi-stage feature
 598 pipeline on timestamped speech transcriptions for dementia assessment. In *ICASSP 2025-2025*
 599 *IEEE International Conference on Acoustics, Speech and Signal Processing (ICASSP)*, pp. 1–2.
 600 IEEE, 2025.

601 Ashish Vaswani, Noam Shazeer, Niki Parmar, Jakob Uszkoreit, Llion Jones, Aidan N Gomez,
 602 Łukasz Kaiser, and Illia Polosukhin. Attention is all you need. *Advances in neural informa-*
 603 *tion processing systems*, 30, 2017.

605 Pingping Wu, Ruihao Wang, Han Lin, Fanlong Zhang, Juan Tu, and Miao Sun. Automatic depres-
 606 sion recognition by intelligent speech signal processing: A systematic survey. *CAAI Transactions*
 607 *on Intelligence Technology*, 8(3):701–711, 2023a.

608 Wen Wu, Chao Zhang, and Philip C Woodland. Self-supervised representations in speech-based
 609 depression detection. In *ICASSP 2023-2023 IEEE International Conference on Acoustics, Speech*
 610 *and Signal Processing (ICASSP)*, pp. 1–5. IEEE, 2023b.

612 Wen Wu, Chao Zhang, and Philip C Woodland. Confidence estimation for automatic detection of de-
 613 pression and alzheimer’s disease based on clinical interviews. *arXiv preprint arXiv:2407.19984*,
 614 2024.

615 Junqi Xue, Ruihan Qin, Xinxu Zhou, Honghai Liu, Min Zhang, and Zhiguo Zhang. Fusing multi-
 616 level features from audio and contextual sentence embedding from text for interview-based de-
 617 pression detection. In *ICASSP 2024-2024 IEEE International Conference on Acoustics, Speech*
 618 *and Signal Processing (ICASSP)*, pp. 6790–6794. IEEE, 2024.

620 Fan Yang, Kai Wu, Shuyi Zhang, Guannan Jiang, Yong Liu, Feng Zheng, Wei Zhang, Chengjie
 621 Wang, and Long Zeng. Class-aware contrastive semi-supervised learning. In *Proceedings of the*
 622 *IEEE/CVF Conference on Computer Vision and Pattern Recognition*, pp. 14421–14430, 2022.

623 Minghui Zhao, Hongxiang Gao, Lulu Zhao, Zhongyu Wang, Fei Wang, Wenming Zheng, Jianqing
 624 Li, and Chengyu Liu. Decoupled multi-perspective fusion for speech depression detection. *IEEE*
 625 *Transactions on Affective Computing*, 2025.

627 Zhiyuan Zhou, Yanrong Guo, Shijie Hao, and Richang Hong. Hierarchical multifeature fusion via
 628 audio-response-level modeling for depression detection. *IEEE transactions on computational*
 629 *social systems*, 10(5):2797–2805, 2022.

631 Maryam Zolnoori, Ali Zolnour, and Maxim Topaz. Adscren: A speech processing-based screening
 632 system for automatic identification of patients with alzheimer’s disease and related dementia.
 633 *Artificial intelligence in medicine*, 143:102624, 2023.

635 A DATASET DETAILS

637 EATD-Corpus (Shen et al., 2022) is a publicly available Chinese depression dataset, which com-
 638 prises audios and text transcripts extracted from the interviews of 162 volunteers. All the volunteers
 639 have signed informed consents and guarantee the authenticity of all the information provided. Each
 640 volunteer is required to answer three randomly selected questions and complete an SDS question-
 641 naire. SDS is a commonly used questionnaire for psychologists to screen depressed individuals in
 642 practice (Shen et al., 2022). The EATD-Corpus consists of 162 samples, totaling 2.26 hours of au-
 643 dio data, which includes 132 samples from healthy controls and 30 from patients diagnosed with
 644 depression. To ensure a fair comparison with prior studies, we employed a 3-fold cross-validation
 645 scheme. We utilized only the audio data, partitioning all samples into three equal folds: two for
 646 training and one for testing. Furthermore, to maintain the stability of the results, we augmented the
 647 test set by reshuffling the data following the methodology of Shen et al. (2022), while the training
 set was kept unchanged. The final results are reported as the average over the three folds.

648 ADReSSo21 (Luz et al., 2021) is a publicly available English-language Alzheimer’s Disease dataset,
649 comprising two subsets for distinct sub-tasks. The dataset is balanced for age and gender and in-
650 cludes audio recordings from both investigators and participants. Each data contains recordings of a
651 picture description task (“Cookie Theft” picture from the Boston Diagnostic Aphasia Exam). Those
652 recordings have been acoustically enhanced (noise reduction through spectral subtraction) and nor-
653 malized. To ensure a fair comparison with prior work, we utilized only the audio data and adhered
654 to the Luz et al. (2021)’s splits for the training and test sets. A validation set was further partitioned
655 from the training set, and the final results are reported on the test set. We conducted multiple ex-
656 perimental runs with different random seeds. Furthermore, as the majority of previous studies have
657 focused on the first sub-task of ADReSSo21, namely the Alzheimer’s Disease classification task, we
658 also provide the results of our method on this sub-task for a direct comparison.
659

660 B TRAINING DETAILS

661 We employed the Adam optimizer with an initial learning rate of 2e-6 and a weight decay of 1e-8.
662 The batch sizes for both labeled and unlabeled data were set to 2, with 4 gradient accumulation steps.
663 The primary data augmentation methods included speed perturbation and time masking. The decay
664 rate for the Exponential Moving Average (EMA) was set to 0.999. For the model architecture,
665 features were extracted from the 10th layer of all audio encoders. The temporal pooling kernel
666 size was set to 5. The transformer model comprised 3 blocks with 16 attention heads, while the
667 RNN model consisted of a 2-layer bidirectional LSTM. Notably, as the EATD-Corpus is a Chinese
668 dataset, we used HuBERT and wav2vec2 models pre-trained on Chinese speech datasets. Due to
669 the unavailability of a WavLM model pre-trained on Chinese data, the version we employed was
670 pre-trained on an English dataset.
671

672 C THE USE OF LARGE LANGUAGE MODELS (LLMs)

673 We disclose that we used Gemini-2.5-Pro to assist in polishing the language and improving the clar-
674 ity of this paper. The model was used for grammar correction, sentence restructuring, and enhanc-
675 ing overall readability. All technical content, experimental design, results, and conclusions were
676 authored and verified solely by the human authors. The LLM did not contribute to the generation of
677 ideas, methods, or data analysis.
678

680
681
682
683
684
685
686
687
688
689
690
691
692
693
694
695
696
697
698
699
700
701